PHYSICAL REVIEW B **106**, L121117 (2022)

Letter

Emergent topological orders and phase transitions in lattice Chern-Simons theory of quantum magnets

Rui Wang,[1,2] Z. Y. Xie,[3,*] Baigeng Wang,[1,2,†] and Tigran Sedrakyan[4]
[1]*National Laboratory of Solid State Microstructures and Department of Physics, Nanjing University, Nanjing 210093, China*
[2]*Collaborative Innovation Center for Advanced Microstructures, Nanjing 210093, China*
[3]*Department of Physics, Renmin University of China, Beijing 100872, China*
[4]*Department of Physics, University of Massachusetts, Amherst, Massachusetts 01003, USA*

(Received 1 February 2021; revised 11 September 2022; accepted 14 September 2022; published 29 September 2022)

Topological phase transitions involving intrinsic topological orders are usually characterized by qualitative changes of ground state quantum entanglement, which cannot be described by conventional mean-field theories with local order parameters. Here, we apply the lattice Chern-Simons theory to study frustrated quantum magnets and show that the conventional concepts, such as the order parameter and symmetry breaking, can still play a crucial role in certain topological phase transitions. The lattice Chern-Simons representation establishes a nonlocal mapping from quantum spin models to interacting spinless Dirac fermions. We show that breaking certain emergent symmetries of the fermionic theory could provide a unified approach to describing both magnetic and topological orders, as well as the topological phase transitions between them. We apply this method to the perturbed spin-1/2 J_1-J_2 XY model on the honeycomb lattice and predict a nonuniform chiral spin liquid ground state in the strong frustration region. This is further verified by our high-precision tensor network calculations. These results suggest that the lattice Chern-Simons theory can simplify the complicated topological phase transitions to effective mean-field theories in terms of fermionic degrees of freedom, which lead to different understandings that help to understand the frustrated quantum magnets.

DOI: 10.1103/PhysRevB.106.L121117

I. INTRODUCTION

Intrinsic topological orders (TOs) [1–3] and topological phase transitions (TPTs) [4–12] have constituted one of the most active fields since the discovery of fractional quantum Hall effect [13–16]. In stark contrast with the conventional long-range orders, the TOs are featured by their ground state degeneracy [17] and the emergence of anyonic excitations [18,19]. Because of these distinct physical natures, it is widely believed that the TPTs are characterized by qualitative changes of systems' quantum entanglement, thus are generally beyond the conventional mean-field theories based on local order parameters.

A prominent example of TOs is the quantum spin liquids (QSLs) stabilized in two-dimensional (2D) quantum magnets under strong frustration [20–25]. They are disordered quantum states with fractionalized excitations. Moreover, they display the emergent gauge fluctuations [26], the key feature of QSLs. In contrast, the gauge fluctuations become unimportant and negligible when magnetic orders are formed under weak frustration. The different behaviors of the gauge degrees of freedom in the two types of phases pose significant challenges to understanding the TPTs between them, which evoked extensive investigations in the last decade [12,27–32]. The main difficulty comes from the different languages used for the QSLs and the magnetic orders. The former is described by fractionalized excitations and emergent gauge fluctuations, while the latter by spin waves or magnons.

In this work, we apply the flux attachment [33–44] to frustrated quantum magnets, and propose a mean-field theory that describes the magnetic orders, QSLs, and the TPTs between them in a unified way. We propose a nonlocal mapping from the quantum spin models to strongly correlated spinless Dirac fermions, as indicated by Figs. 1(a) and 1(b). This mapping is based on the lattice Chern-Simons (CS) representation of hard-core bosons, a lattice version of the flux attachment. When applied to frustrated quantum magnets, some symmetries implicit in the original spin basis [45,46] can emerge in the Dirac fermion system. Moreover, breaking these emergent symmetries leads to mean-field descriptions not only for the magnetic orders but also for certain QSLs.

More specifically, breaking the emergent symmetries results in different fermion orders that gap out the Dirac nodes. Although these orders describe short-range entangled states in the fermion basis, they could characterize certain TOs with long-range quantum entanglement in the original spin basis, since the two bases are related to each other by a nonlocal transformation. Particularly, we show that the superconducting phase in the fermion basis corresponds to the planar Néel antiferromagnetic order (AFM) in the spin language [Fig. 1(c)], and the topological excitonic phase formed by the fermions essentially describes the chiral spin liquids (CSLs) with semionic excitations [Fig. 1(d)]. We further apply our scheme to study the perturbed spin-1/2 J_1-J_2 XY model on

---

[*] qingtaoxie@ruc.edu.cn

[†] bgwang@nju.edu.cn

©2022 American Physical Society

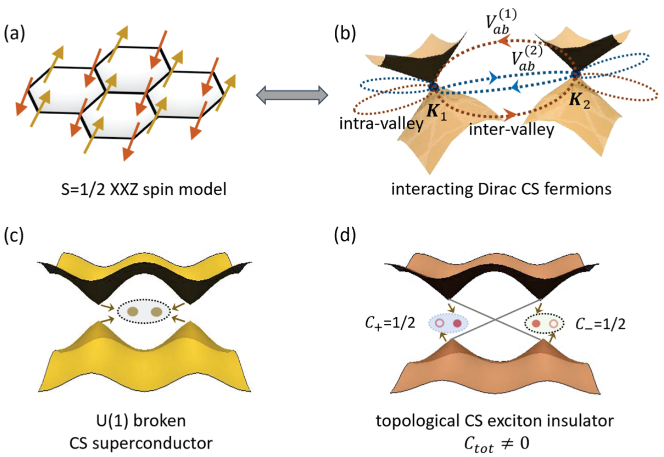

FIG. 1. The lattice CS representation of a quantum spin model. The spin-1/2 XXZ models (a) are mapped in low energy to a system of spinless Dirac fermions with inter- and intravalley interactions (b). The interactions can favor different fermion orders. For example, the Dirac fermions can form Cooper pairs, leading to the CS superconductor as shown in (c). The Dirac fermions can also form particle-hole pairs, generating a topological CS exciton insulator with nonzero total Chern number, as indicated by (d).

the honeycomb lattice. A TPT from the planar Néel AFM to a nonuniform CSL [37] is found, which is further confirmed by our tensor network calculations [47–52]. These results suggest possibilities to unify the magnetic orders and QSLs in simple mean-field theories after properly implementing the lattice CS theory, which could be useful to explore novel phases and unconventional phase transitions in frustrated quantum magnets.

II. LATTICE CS THEORY OF QUANTUM MAGNETS

A. Mapping to fermionic theory

We start from the general quantum spin XXZ model

$$H_{XXZ} = \sum_{\mathbf{r},\mathbf{r}'} (J_{\mathbf{r},\mathbf{r}'}/2)(\hat{S}^+_{\mathbf{r}}\hat{S}^-_{\mathbf{r}'} + \hat{S}^-_{\mathbf{r}}\hat{S}^+_{\mathbf{r}'}) + J^z_{\mathbf{r},\mathbf{r}'}\hat{S}^z_{\mathbf{r}}\hat{S}^z_{\mathbf{r}'}, \qquad (1)$$

where $\hat{S}^{\pm}_{\mathbf{r}}$ is the spin-raising/lowering operator at site $\mathbf{r}$. $J_{\mathbf{r},\mathbf{r}'}, J^z_{\mathbf{r},\mathbf{r}'} > 0$ and they involve couplings up to the nth nearest neighbor (NN), forming the n-dimensional vectors $\mathbf{J} = (J_1, J_2, \dots, J_n)$, $\mathbf{J}^z = (J^z_1, J^z_2, \dots, J^z_n)$.

The spin-raising and lowering operators, $S^{\pm}_{\mathbf{r}}$, of Eq. (1) are statistically equivalent to hard-core bosons. Instead of resorting to the parton representations, we write $S^{\pm}_{\mathbf{r}}$ into spinless fermions. This is desirable since Pauli's principle automatically prohibits double occupancy. In addition, to enforce the bosonic mutual statistics, a flux quanta must be attached to each fermion as in Fig. 2(a). This constitutes an exact representation of the elementary spin excitations [53].

It is well known that the flux attachment can be naturally achieved by coupling the fermions to CS gauge field A_μ [70,71], with the action

$$S_{SC} = \frac{1}{4\pi}\int d^3r\,\epsilon^{\mu\nu\rho}A_\mu\partial_\nu A_\rho. \qquad (2)$$

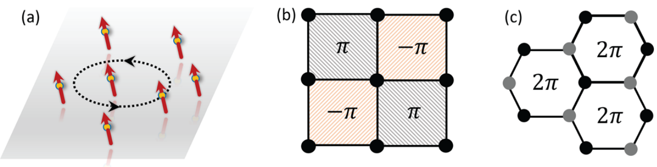

FIG. 2. (a) The spin-raising/lowering operators are represented by spinless fermions attached to a flux quanta. (b),(c) With neglecting gauge fluctuations, the π-flux (2π-flux) phase is found stable on square (honeycomb) lattice. Consequently, spinless Dirac fermions emerge in low energy as in Fig. 1(b).

For the quantum spin models in Eq. (1), the gauge field essentially arises from the spin-spin exchange interactions. This motivates us to introduce the following nonlocal transformation between the spin and fermion basis [37–40], $\hat{S}^{\pm}_{\mathbf{r}} = f^{\pm}_{\mathbf{r}}U^{\pm}_{\mathbf{r}}$, where $f^{\pm}_{\mathbf{r}}$ are creation/annihilation operators of the spinless fermions. $U^{\pm}_{\mathbf{r}} = \exp[\pm ie\sum_{\mathbf{r}'\neq\mathbf{r}}\arg(\mathbf{r}-\mathbf{r}')n_{\mathbf{r}'}]$ are nonlocal string operators, where $n_{\mathbf{r}}$ denotes the particle number operator at site $\mathbf{r}$, and e is the CS charge that takes value of odd integers [37–39].

Inserting the nonlocal transformation to Eq. (1), we arrive at a system of spinless fermions coupled to the CS gauge field A_μ. In addition, the fermions are subject to local repulsive interactions, originated from the Ising terms $J^z_{\mathbf{r},\mathbf{r}'}$ in Eq. (1). We firstly neglect the gauge fluctuations. Then, the spinless fermions effectively move on the lattice with a flux background. The flux can be self-consistently determined by minimizing the system energy. For example, π-flux and 2π-flux phases can be obtained [72] on square and honeycomb lattice, respectively, as shown by Figs. 2(b) and 2(c). Consequently, spinless Dirac fermions emerge in low energy, located at different valleys in momentum space as in Fig. 1(b). Due to the vanishing density of states of the Dirac fermions, the interactions arising from the $J^z_{\mathbf{r},\mathbf{r}'}$ terms are irrelevant for $J^z_{\mathbf{r},\mathbf{r}'} \lesssim J_{\mathbf{r},\mathbf{r}'}$.

After restoring the gauge fluctuations coupled to the Dirac fermions, we generally obtain [53]

$$S = \sum_{a=1}^{N}\int d^3r\, f^\dagger_{a,r} i\not{D} f_{a,r} + S_{CS} + \dots, \qquad (3)$$

where $\not{D} = \sigma^\mu(i\partial_\mu - eA_\mu)$, with $\mu = 0, 1, 2$, and σ_μ is the Pauli matrix defined in the sublattice space. $r = (t, \mathbf{r})$, $f_a = [f_{a,A,r}, f_{a,B,r}]^{\mathrm{T}}$ is a Dirac spinor, where $a = 1, 2, \dots, N$ denotes the N Dirac valleys located at the momentum $\mathbf{K}_a$ [38]. The ellipsis denotes the terms that generate higher-order dispersions, which are negligible near the Dirac points.

The advantages of the CS representation over the parton representations are implicit in Eq. (3). First, the gauge field here does not introduce any projective symmetries [26], since the CS representation does not enlarge the Hilbert space. Second, in analogy with the photon-induced electron-electron interaction in quantum electrodynamics, the CS gauge field can induce interactions between the Dirac fermions [70]. Integrating out A_μ formally leads to

$$H_f = \sum_{a=1}^{N}\int d\mathbf{r}\, f^\dagger_{a,\mathbf{r}}\boldsymbol{\sigma}^{(a)}\cdot(-i\nabla)f_{a,\mathbf{r}} + \sum_{i=1}^{M} w_i(\mathbf{J})V^{(i)}_{\mathrm{int}}, \qquad (4)$$

where $V_{\rm int}^{(i)}$, with $i = 1, 2, \ldots, M$, are M-induced interactions, which are nonlocal and model dependent. The weight of the ith interaction, $\omega_i(\mathbf{J})$, relies on $\mathbf{J}$. We note that both inter- and intravalley interactions can be generated, as indicated by Fig. 1(b). The fermionic theory in Eq. (4) describes the low-energy physics of the spin model in Eq. (1). In addition, Eq. (4) enjoys the emergent gauge U(1) and the sublattice symmetry, which are implicit in Eq. (1).

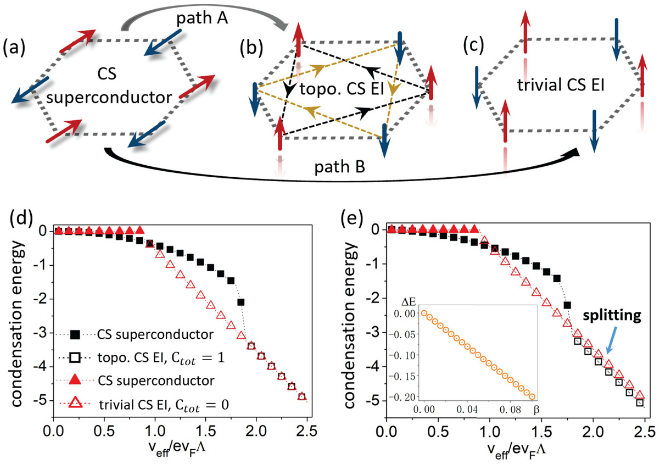

FIG. 3. (a)–(c) Typical fermion orders and phase transitions predicted for the J_1-J_2 XY model. With increasing frustration, a TPT from a CS superconductor to EIs is found, with two possible transition paths, A and B, leading to the topological and trivial EI, respectively. (d) The condensation energy of the unperturbed XY model as a function of $v_{\rm eff}$, calculated for path A (the black data curve) and B (the red data curve). (e) The condensation energy with a flux perturbation of strength β. The energy splitting is found for large $v_{\rm eff}$, and the topological EI becomes more stable under perturbation. The inset shows the energy difference between the two EIs, ΔE, as a function of β, where $v_{\rm eff}/ev_F\Lambda = 2.3$.

B. CS superconductors and CS excitonic insulators

It is known that strong nonlocal interactions can gap out the Dirac semimetals [67,73], resulting in different types of long-range orders. By analogy, fermion orders can spontaneously take place in Eq. (4). Furthermore, since Eq. (4) is derived in a nonlocal basis after CS transformation, one expects that the fermion orders may capture the long-range entanglement features of certain TOs in the original spin basis. We now focus on two types of fermion orders, which break the two above-mentioned emergent symmetries.

First, with breaking the emergent gauge U(1) symmetry, the Dirac fermions form Cooper pairs, resulting in the CS superconductors, as indicated by Fig. 1(c). Such paired states are always found stable when the system has weak frustration [38–40]. Interestingly, the CS superconductors exhibit physical correspondence with planar Néel AFMs. For example, the two states share quantitatively the same excitations, such as the low-energy Goldstone modes and Higgs modes [38,40].

It should be noted that the CS superconductor has conceptual analogy with the condensation of Schwinger bosons. In the Schwinger boson representation, the magnetic orders can be understood as condensed Schwinger bosons [74]. Here, the condensation of paired f fermions also generates magnetic orders. In addition, we also remark that the CS superconductors are distinct in nature from the normal superconductors. In the traditional BCS theory, while the U(1) is Higgsed, the remnant Bogoliubov–de Gennes (BdG) Hamiltonian still has the fermion parity symmetry, leading to a Z_2 topological order. However, the situation of the CS superconductor is different, and the gauge U(1) here is completely broken. The self-consistent mean-field solution of the CS superconductors [38] exists only in the form of a completely U(1) gauge symmetry broken BdG Hamiltonian from the DIII symmetry class (which is a symmetry protected topological state) with certain self-consistency relations. Therefore, the CS superconductors have no Z_2 topological order.

Second, the Dirac fermions can also be gapped out by the spontaneous formation of excitons, i.e., particle-hole pairs, leading to CS exciton insulators (EIs). From Eq. (4), the mean-field Hamiltonian for these states can be derived in low energy as $H_a^{EI} = v_F(k_x\sigma^x + k_y\sigma^y) + \chi_a\sigma^z$, where χ_a is the exciton mass for the ath Dirac fermion. Such states break the emergent sublattice symmetry for the Dirac fermions, generating an out-of-plane Néel AFM in the spin language. For these states, each of the massive Dirac fermions exhibits the Chern number $C_a = {\rm sgn}(\chi_a)/2$, and the total Chern number is given by $C_{\rm tot} = \sum_{a=1}^{N} C_a$. We now consider the case with two massive Dirac fermions of the same Chern number 1/2, thus $C_{\rm tot} = 1$. As shown in Fig. 1(d), this constitutes a topological CS exciton insulator with spontaneous breaking of the time-reversal symmetry (TRS). In real space, the TRS breaking is essentially attributed to the CS gauge flux coupled to the fermions, as indicated by the staggering flux in Fig. 3(b). Clearly, this is a close analogy with the Haldane's Chern insulator on honeycomb lattice [75]. With going beyond the mean-field theory, the fluctuation of the exciton order is described by a CS field theory with the coefficient $C_{\rm tot}/4\pi$ [71,76]. In addition, the fermions are further coupled to the CS gauge field given by Eq. (2). Therefore, the total effective field theory reads as

$$S_{EI} = \frac{k}{4\pi}\int d^3r\,\epsilon^{\mu\nu\rho}A_\mu\partial_\nu A_\rho, \qquad (5)$$

where $k = 2$. This implies the emergence of semionic excitations, a smoking-gun feature of the Kalmeyer-Laughlin CSL [77]. Therefore, with breaking the emergent sublattice and time-reversal symmetry, the resulting topological CS exciton insulator essentially describes a nonuniform CSL originally proposed in Ref. [37], which is a coexistence of CSL and the out-of-plane Néel AFM.

Similarly, when the system breaks the emergent sublattice symmetry while respecting the TRS, a topologically trivial CS exciton insulator with $C_{\rm tot} = 0$ will be generated. This nontopological phase has a staggered chemical potential for the fermions on different sublattices, and thus will display a trivial out-of-plane Néel AFM order in the spin basis, as shown by Fig. 3(c).

So far, we have shown that the fermion orders efficiently describe corresponding phases in the original spin basis. Importantly, this scheme can significantly simplify our understanding of TPTs. For example, the TPT from the planar Néel AFM to the nonuniform CSL is now translated into the transition between the CS superconductor and the topological CS exciton insulator.

III. A CONCRETE APPLICATION: THE PERTURBED J_1-J_2 XY HONEYCOMB MODEL

A. CS mean-field theory

We now explicitly discuss an application of the proposed scheme by studying the J_1-J_2 XY model on the honeycomb lattice, with a staggered-flux perturbation of strength β, as shown by Fig. 3(b). For the pure XY model, an intermediate phase with an unexpected out-of-plane Néel AFM order [68,78,79] has been numerically observed [68,78–81]. The physical mechanism for this intermediate phase still remains unclear.

We firstly consider the unperturbed case with $\beta = 0$. After applying the CS transformation, we arrive at a low-energy fermionic theory [53], $H_{\mathrm{tot}} = \sum_{a=\pm} H_{0,a} + V_{\mathrm{int}}^{(1)} + V_{\mathrm{int}}^{(2)}$, where

$$H_{0,a} = \sum_{\mathbf{k}} f_{a,\mathbf{k}}^{\dagger} a v_F \mathbf{k} \cdot \boldsymbol{\sigma}^{(a)} f_{a,\mathbf{k}} \tag{6}$$

describes low-energy Dirac fermions with a momentum cutoff Λ. The two valleys are denoted by $a = \pm$ and $\boldsymbol{\sigma}^{(+)} = \boldsymbol{\sigma}$, $\boldsymbol{\sigma}^{(-)} = \boldsymbol{\sigma}^{\mathrm{T}}$. $v_F = \sqrt{3}\epsilon J_1/2$, and ϵ is the lattice constant.

For $J_1 \gg J_2$, i.e., the weak frustration case, the dominant fermion-fermion interaction is obtained as

$$V_{\mathrm{int}}^{(1)} = \sum_{\mathbf{k}_1,\mathbf{k}_2,\mathbf{q}} v_{\mathbf{q}}^{\alpha\beta\rho\lambda} f_{a,\alpha,\mathbf{k}_1}^{\dagger} f_{a,\beta,\mathbf{k}_1+\mathbf{q}} f_{\bar{a},\rho,\mathbf{k}_2}^{\dagger} f_{\bar{a},\lambda,\mathbf{k}_2-\mathbf{q}}, \tag{7}$$

where $v_{\mathbf{q}}^{\alpha\beta\rho\lambda} = -ev_F(\sigma_{\alpha\lambda}^{i}\delta_{\beta\rho} + \delta_{\alpha\lambda}\sigma_{\beta\rho}^{iT})A_{\mathbf{q}}^{j}$, with $A_{\mathbf{q}}^{j} = 2\pi i\epsilon^{ij}q^{j}/q^{2}$, ϵ^{ij} being the Levi-Civita tensor. Moreover, with increasing J_2/J_1, we observe the growth of another interaction,

$$V_{\mathrm{int}}^{(2)} = v_{\mathrm{eff}} \sum_{\mathbf{k}_1,\mathbf{k}_2,\mathbf{q}} f_{a,\alpha,\mathbf{k}_1}^{\dagger} f_{a,\alpha,\mathbf{k}_1+\mathbf{q}} f_{b,\beta,\mathbf{k}_2}^{\dagger} f_{b,\beta,\mathbf{k}_2-\mathbf{q}}, \tag{8}$$

where $v_{\mathrm{eff}} = 2\pi^2/m^2\Lambda v_F$ and $m = 2/3eJ_2$.

For $V_{\mathrm{int}}^{(2)} \ll V_{\mathrm{int}}^{(1)}$, we find that the CS superconductor is stabilized, with a nontrivial SC order parameter Δ_3 being developed, as also proved by our previous works [38–40]. For $V_{\mathrm{int}}^{(2)} \gg V_{\mathrm{int}}^{(1)}$, we perform a detailed renormalization group analysis followed by self-consistent mean-field calculations [53]. We show that the s-wave intravalley EIs are most stable. Consequently, the exciton mass χ_a is generated for the ath valley. Moreover, it is found that the corresponding mean-field energy does not rely on the sign of χ_a. Thus, two different types of EI may emerge as closely competing ground states, with $C_{\mathrm{tot}} = 0$ and $C_{\mathrm{tot}} = 1$, respectively, which are energetically degenerate in mean-field level.

So far, our approach predicts a transition from CS superconductor to EI with increasing J_2/J_1 (proportional to $V_{\mathrm{int}}^{(2)}/V_{\mathrm{int}}^{(1)}$). In addition, because of the energy degeneracy of the $C_{\mathrm{tot}} = 0$ and $C_{\mathrm{tot}} = 1$ states for $V_{\mathrm{int}}^{(2)}/V_{\mathrm{int}}^{(1)} \gg 1$, two transition paths are possible, as shown by Figs. 3(a)–3(c). Based on the above scheme, both the paths enjoy the mean-field description as

$$H_{\mathrm{tot}}^{(m)} = v_F \mathbf{k} \cdot \boldsymbol{\sigma} \tau^{z} + \hat{\Delta}_{\mathbf{k}} \tau^{+} + \hat{\Delta}_{\mathbf{k}}^{\dagger} \tau^{-} + \chi \tau^{(m)} \sigma^{z}, \tag{9}$$

where we have introduced the Nambu-sublattice basis, $\Psi_{\mathbf{k}} = [f_{a,A,\mathbf{k}}, f_{a,B,\mathbf{k}}, f_{\bar{a},A,-\mathbf{k}}^{\dagger}, f_{\bar{a},B,-\mathbf{k}}^{\dagger}]^{\mathrm{T}}$. The upper index $m = A, B$ denotes the two transition paths, and we defined $\tau^{(A)} = \tau^{0}$, $\tau^{(B)} = \tau^{z}$. $\hat{\Delta}_{\mathbf{k}}$ is the superconductor order parameter in the sublattice space [53]. Clearly, Eq. (9) describes the transitions between the CS superconductor and EIs.

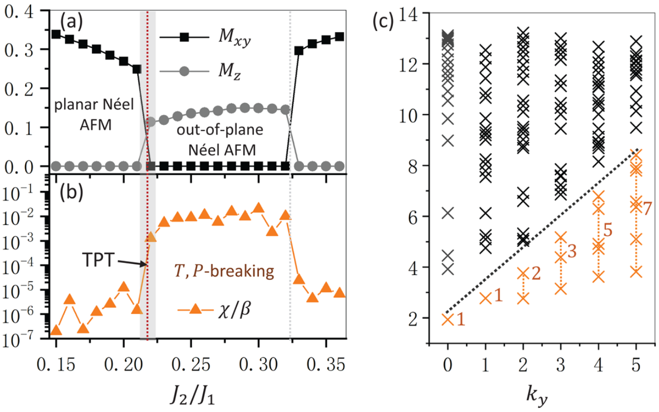

FIG. 4. The tensor network results for $D = 12$, $\beta = 0.01$. (a) The planar Néel AFM order is stable for $J_2/J_1 \lesssim 0.22$ with nonzero M_{xy} defined by $M_{xy} = \sum_{\mathbf{r}} \sqrt{M_{\mathbf{r},x}^2 + M_{\mathbf{r},y}^2}/N$. After crossing the TPT (the shaded region), an intermediate state is found, displaying an out-of-plane Néel AFM order, i.e., $M_z = \sum_{\mathbf{r}} |M_{\mathbf{r},z}|/N \neq 0$. A subsequent phase transition takes place at larger J_2/J_1, which is not the focus of this work. (b) The chirality order $\chi = \langle \hat{S}_{\mathbf{r}_1} \times (\hat{S}_{\mathbf{r}_2} \cdot \hat{S}_{\mathbf{r}_3}) \rangle$ is evaluated in each triangle from one sublattice. It displays a much larger value in the intermediate phase. (c) The entanglement spectrum obtained from a cut in an infinite cylinder with six unit cells along L_y. $J_2/J_1 = 0.3$ and k_y is in units of $\pi/3$.

Figure 3(d) shows the self-consistently calculated condensation energy versus v_{eff} for each path. With increasing v_{eff}, the system firstly stabilizes the CS superconductor (Néel AFM state). It then evolves into a trivial CS exciton insulator (out-of-plane Néel order). For even larger v_{eff}, the energy of the $C_{\mathrm{tot}} = 0$ and $C_{\mathrm{tot}} = 1$ EI state become indistinguishable in mean-field level, indicating that these two states are strongly competing under strong frustration.

We now further consider the effect of the staggered-flux perturbation with finite β. As shown by Fig. 3(e), an energy splitting takes place for large v_{eff} under strong frustration, and the topological EI (nonuniform CSL) has the lower energy. Moreover, this state becomes more and more stable with larger β, as shown by the inset to Fig. 3(e). As a result, we predict that a novel phase transition from the planar Néel AFM to the nonuniform CSL can be induced by the perturbation.

B. Numerical evidences

We now present the tensor network results on the J_1-J_2 XY model with the flux perturbation $\beta = 0.01$. We use imaginary-time evolution to determine the ground state [53] that is represented as the projected entangled simplex state ansatz [69,82]. As shown by Fig. 4(a), an intermediate phase is found in $J_2/J_1 \sim (0.22, 0.33)$, which is disordered in the XY plane but displays an out-of-plane Néel AFM order. More interestingly, as shown by Fig. 4(b), we observe a significant enhancement of the chirality for $J_2/J_1 \sim (0.22, 0.33)$, indicating $\mathcal{T}, \mathcal{P}$ breaking of the intermediate phase. The entanglement spectrum is also shown by Fig. 4(c), where a nontrivial degeneracy $1, 1, 2, 3, 5, \ldots$ is obtained, which is consistent with $SU(2)_1$ Wess-Zumino-Novikov-Witten conformal field theory [83], suggesting the existence of chiral edge state. All these numerical findings are in support of our analytic predictions, indicating a TPT from planar Néel order to the nonuniform CSL.

We have also calculated the J_1-J_2 honeycomb XY model with turning off β. The out-of-plane Néel AFM as that in Fig. 4(a) can still be obtained for $J_2/J_1 \sim (0.22, 0.33)$. However, the chirality order in this region becomes vanishingly small, in agreement with previous numerical studies [68,78,79]. Moreover, in contrast with the case of $\beta = 0.01$, we also calculated the entanglement spectrum for $\beta = 0$ but no clear signature of spectrum degeneracy can be found. The sharp difference between the unperturbed ($\beta = 0$) and weakly perturbed ($\beta = 0.01$) case suggests that the J_1-J_2 honeycomb XY model is highly sensitive to perturbations. This can be understood from the field theoretical calculations in Fig. 3(d), which indicate that there is accidental degeneracy between the trivial (conventional out-of-plane AFM order) and the topological CS exciton insulator (nonuniform CSL). Thus, with introducing a weak staggered-flux perturbation β, the nonuniform CSL wins in energetics and emerges as the ground state, as indicated by Fig. 3(e).

We remark that the ground state seems to rely on the specific forms of perturbation as well. For example, with the staggered-flux perturbation β, both Ref. [78] and our calculations observe finite chirality order for $J_2/J_1 \sim (0.22, 0.33)$. The latter is, however, absent if one instead introduces the chiral term perturbation J_χ [79]. The different responses to different perturbations in fact reflect the nonuniform nature of the CSL. In the latter phase, the out-of-plane AFM Ising order is locked to the chirality χ, and they occur simultaneously. Thus, the nonuniform CSL could only be stabilized by those perturbations that favor both the out-of-plane order and the chirality. This is in key distinction with the conventional CSL induced by the chiral term J_χ [79]. Although J_χ breaks TRS, it does not favor the out-of-plane AFM order. Therefore, this perturbation cannot generate nonuniform CSL as it could not lift the accidental degeneracy in Fig. 3(d).

IV. CONCLUSION AND DISCUSSION

This work reveals a systematic approach to investigate TPTs in frustrated quantum magnets. This is achieved by first adopting the lattice CS representation and then integrating the CS gauge fluctuations. Then, we show that certain TPTs can be captured by elegant mean-field theories of the mapped interacting fermionic model. As a prototypical example, the perturbed J_1-J_2 XY model on the honeycomb lattice is carefully analyzed. For this model, we predict a TPT from planar Néel AFM to nonuniform CSL. Large-scale tensor network calculations also support this. Finally, an unconventional mean-field picture is achieved that describes the TPT: a transition from a CS superconductor to a topological CS exciton insulator.

It should be noted that our method constitutes a general approach to predict possible phases and analyze TPTs. Indeed, the fermion orders proposed here can be generalized to describe other exotic phases, such as helical Dirac spin liquid [44], U(1) Dirac [84], and Z_2 spin liquid. As a result, we expect the proposed CS mean-field theory to describe different types of TPTs. Moreover, our method has some advantages over previous methods. First, it does not require notions such as the higher-form symmetries [85–87]; the current framework uses conventional notions of symmetry breaking. Second, it could uncover some hidden features of TOs and build connections between the TOs and some familiar fermionic states.

Another research direction that arises from the present work is the possible classification of spin liquids based on dualities and general Chern-Simons flux attachment. Spin-liquid states have been classified in many systems, mainly when the SU(2) spin-rotation symmetry is conserved. Classifications of spin liquids have been performed for various lattices using Schwinger-boson and Abrikosov-fermion representations. Previous works also used the projective symmetry group method to classify Z_2 [26] and chiral spin liquids [88]. However, exhaustive classification of possible quantum spin liquids on a given lattice model with topological field theories and physical properties is still lacking.

Here one can develop a classification scheme of spin liquids based on all possible Chern-Simons flux attachment representations of spin operators. Using these representations, we will not only resort to flux smearing approximation, as usually done for chiral spin liquids, but we will look for the realization of combinations of mutual Chern-Simons terms upon performing different flux attachments on different sublattices. One can also look for a breakdown of Chern-Simons superconductivity yielding a variety of possible Dirac spin liquids and states supporting couplings to a larger number of gauge degrees of freedom. This task will inform about the nature of possible excitations, the nature of emergent gauge fields, and all the symmetries of the state. The result can also be compared with (and, when applicable, recover) the projective group classification of the spin liquids.

Because this method does not require the SU(2) symmetry of the Hamiltonian, it can generate a variety of gapless spin liquids that are beyond the reach of methods requiring the SU(2) symmetry. Such an example is shown in Ref. [44], where a novel helical spin liquid with $N = 6$ anisotropic Dirac cones and with nonzero vector chirality yielding a broken Z_2 symmetry was proposed. Moreover, a continuous quantum phase transition to a 120°-ordered state was studied. Another advantage of this classification scheme is that there are no constraint issues in the Chern-Simons classification scheme as opposed to the Schwinger scheme, where one needs to introduce a constraint to remove extra degrees of freedom.

ACKNOWLEDGMENTS

We acknowledge Qianghua Wang, Xiaoqun Wang, Yixuan Huang, and Hong-Hao Tu for helpful discussions. This work was supported by the National Natural Science Foundation of China (Grants No. 11904225, No. 11774420, No. 12274458, and No. 12274206) and the National Key

R&D Program of China (Grants No. 2017YFA0302900, No. 2017YFA0303200, and No. 2016YFA0300503). T.A.S. acknowledges startup funds from UMass Amherst. Z.Y.X. acknowledges the hospitality and support of TDLI.

---

[1] X. G. Wen, Adv. Phys. **44**, 405 (1995).
[2] X. Chen, Z.-C. Gu, and X.-G. Wen, Phys. Rev. B **82**, 155138 (2010).
[3] M. Levin and X.-G. Wen, Phys. Rev. Lett. **96**, 110405 (2006).
[4] T. Senthil, L. Balents, S. Sachdev, A. Vishwanath, and M. P. A. Fisher, Phys. Rev. B **70**, 144407 (2004).
[5] M. Levin and T. Senthil, Phys. Rev. B **70**, 220403(R) (2004).
[6] A. Vishwanath, L. Balents, and T. Senthil, Phys. Rev. B **69**, 224416 (2004).
[7] T. Senthil and M. P. A. Fisher, Phys. Rev. B **74**, 064405 (2006).
[8] A. W. Sandvik, Phys. Rev. Lett. **98**, 227202 (2007).
[9] A. Nahum, P. Serna, J. T. Chalker, M. Ortuño, and A. M. Somoza, Phys. Rev. Lett. **115**, 267203 (2015).
[10] Y. Qi and Z.-C. Gu, Phys. Rev. B **89**, 235122 (2014).
[11] C. Xu and S. Sachdev, Phys. Rev. B **79**, 064405 (2009).
[12] A. Thomson and S. Sachdev, Phys. Rev. X **8**, 011012 (2018).
[13] K. v. Klitzing, G. Dorda, and M. Pepper, Phys. Rev. Lett. **45**, 494 (1980).
[14] R. B. Laughlin, Phys. Rev. Lett. **50**, 1395 (1983).
[15] D. C. Tsui, H. L. Stormer, and A. C. Gossard, Phys. Rev. Lett. **48**, 1559 (1982).
[16] F. D. M. Haldane, Phys. Rev. Lett. **51**, 605 (1983).
[17] X. G. Wen and Q. Niu, Phys. Rev. B **41**, 9377 (1990).
[18] F. Wilczek, Phys. Today **45** (2), 101 (1992).
[19] A. Kitaev, Ann. Phys. **321**, 2 (2006).
[20] P. W. Anderson, Mater. Res. Bull. **8**, 153 (1973).
[21] L. Savary and L. Balents, Rep. Prog. Phys. **80**, 016502 (2017).
[22] P. W. Anderson, Science **235**, 1196 (1987).
[23] L. Balents, Nature (London) **464**, 199 (2010).
[24] P. A. Lee, N. Nagaosa, and X.-G. Wen, Rev. Mod. Phys. **78**, 17 (2006).
[25] B. Normand, Contemp. Phys. **50**, 533 (2009).
[26] X. G. Wen, Phys. Rev. B **65**, 165113 (2002).
[27] S. D. Huber and E. Altman, Phys. Rev. B **82**, 184502 (2010).
[28] C. N. Varney, K. Sun, M. Rigol, and V. Galitski, Phys. Rev. B **84**, 241105(R) (2011).
[29] B. Zhao, J. Takahashi, and A. W. Sandvik, Phys. Rev. Lett. **125**, 257204 (2020).
[30] N. Ma, Y.-Z. You, and Z. Yang Meng, Phys. Rev. Lett. **122**, 175701 (2019).
[31] X.-Y. Song, C. Wang, A. Vishwanath, and Y.-C. He, Nat. Commun. **10**, 4254 (2019).
[32] C. Wang, A. Nahum, M. A. Metlitski, C. Xu, and T. Senthil, Phys. Rev. X **7**, 031051 (2017).
[33] D. M. Gangardt and G. V. Shlyapnikov, Phys. Rev. Lett. **90**, 010401 (2003).
[34] A. Lopez, A. G. Rojo, and E. Fradkin, Phys. Rev. B **49**, 15139 (1994).
[35] K. Yang, L. K. Warman, and S. M. Girvin, Phys. Rev. Lett. **70**, 2641 (1993).
[36] O. Türker and K. Yang, Phys. Rev. B **105**, 155150 (2022).
[37] T. A. Sedrakyan, L. I. Glazman, and A. Kamenev, Phys. Rev. Lett. **114**, 037203 (2015).
[38] R. Wang, B. Wang, and T. Sedrakyan, Phys. Rev. B **105**, 054404 (2022).
[39] T. A. Sedrakyan, V. M. Galitski, and A. Kamenev, Phys. Rev. B **95**, 094511 (2017).
[40] R. Wang, B. Wang, and T. A. Sedrakyan, Phys. Rev. B **98**, 064402 (2018).
[41] S. Maiti and T. Sedrakyan, Phys. Rev. B **99**, 174418 (2019).
[42] S. Maiti and T. A. Sedrakyan, Phys. Rev. B **100**, 125428 (2019).
[43] T. A. Sedrakyan, L. I. Glazman, and A. Kamenev, Phys. Rev. B **89**, 201112(R) (2014).
[44] T. A. Sedrakyan, R. Moessner, and A. Kamenev, Phys. Rev. B **102**, 024430 (2020).
[45] E. Berg, E. G. Dalla Torre, T. Giamarchi, and E. Altman, Phys. Rev. B **77**, 245119 (2008).
[46] E. G. Dalla Torre, E. Berg, and E. Altman, Phys. Rev. Lett. **97**, 260401 (2006).
[47] Z. Y. Xie, J. Chen, M. P. Qin, J. W. Zhu, L. P. Yang, and T. Xiang, Phys. Rev. B **86**, 045139 (2012)
[48] B.-X. Zheng, Chia-Min Chung, P. Corboz, G. Ehlers, Ming-Pu Qin, R. M. Noack, H. Shi, S. R. White, S. Zhang, and G. Kin-Lic Chan, Science **358**, 1155 (2017).
[49] P. Corboz, T. M. Rice, and M. Troyer, Phys. Rev. Lett. **113**, 046402 (2014).
[50] P. Corboz and F. Mila, Phys. Rev. Lett. **112**, 147203 (2014).
[51] L. Wang, Z. C. Gu, F. Verstraete, and X. G. Wen, Phys. Rev. B **94**, 075143 (2016).
[52] H. J. Liao, Z. Y. Xie, J. Chen, Z. Y. Liu, H. D. Xie, R. Z. Huang, B. Normand, and T. Xiang, Phys. Rev. Lett. **118**, 137202 (2017).
[53] See Supplemental Material at http://link.aps.org/supplemental/10.1103/PhysRevB.106.L121117 for pertinent technical details on relevant proofs and derivations, which includes Refs. [3,38,49,54–69].
[54] R.-Z. Huang, H.-J. Liao, Z.-Y. Liu, H.-D. Xie, Z.-Y. Xie, H.-H. Zhao, J. Chen, and T. Xiang, Chin. Phys. B **27**, 070501 (2018).
[55] R. Orús and G. Vidal, Phys. Rev. B **80**, 094403 (2009).
[56] J. I. Cirac, D. Poilblanc, N. Schuch, and F. Verstraete, Phys. Rev. B **83**, 245134 (2011).
[57] M. Lubasch, J. I. Cirac, and M. C. Banuls, Phys. Rev. B **90**, 064425 (2014).
[58] D. Poilblanc, N. Schuch, and I. Affleck, Phys. Rev. B **93**, 174414 (2016).
[59] S. S. Jahromi, R. Orus, M. Kargarian, and A. Langari, Phys. Rev. B **97**, 115161 (2018).
[60] H. C. Jiang, Z. Y. Weng, and T. Xiang, Phys. Rev. Lett. **101**, 090603 (2008).
[61] A. Kitaev and J. Preskill, Phys. Rev. Lett. **96**, 110404 (2006).
[62] G. Vidal, Phys. Rev. Lett. **98**, 070201 (2007).
[63] J. Eisert, M. Cramer, and M. B. Plenio, Rev. Mod. Phys. **82**, 277 (2010).
[64] T. Nishino and K. Okunishi, J. Phys. Soc. Jpn. **65**, 891 (1996).

[65] G. W. Stewart, SIAM J. Matrix Anal. Appl. **23**, 601 (2002).

[66] J.-Y. Chen, J.-W. Li, P. Nataf, S. Capponi, M. Mambrini, K. Totsuka, H.-H. Tu, A. Weichselbaum, J. von Delft, and D. Poilblanc, Phys. Rev. B **104**, 235104 (2021).

[67] R. Wang, O. Erten, B. Wang, and D. Y. Xing, Nat. Commun. **10**, 210 (2019).

[68] Z. Zhu, D. A. Huse, and S. R. White, Phys. Rev. Lett. **111**, 257201 (2013).

[69] Z. Y. Xie, J. Chen, J. F. Yu, X. Kong, B. Normand, and T. Xiang, Phys. Rev. X **4**, 011025 (2014).

[70] A. Altland and B. Simons, *Condensed Matter Field Theory* (Cambridge University Press, Cambridge, UK, 2006).

[71] Gerald V. Dunne, Aspects of Chern-Simons theory, arXiv:hep-th/9902115.

[72] Elliott H. Lieb, Phys. Rev. Lett. **73**, 2158 (1994).

[73] H. Wei, S.-P. Chao, and V. Aji, Phys. Rev. Lett. **109**, 196403 (2012).

[74] S. Sarker, C. Jayaprakash, H. R. Krishnamurthy, and M. Ma, Phys. Rev. B **40**, 5028 (1989).

[75] F. D. M. Haldane, Phys. Rev. Lett. **61**, 2015 (1988).

[76] A. N. Redlich, Phys. Rev. Lett. **52**, 18 (1984).

[77] V. Kalmeyer and R. B. Laughlin, Phys. Rev. Lett. **59**, 2095 (1987).

[78] K. Plekhanov, I. Vasić, A. Petrescu, R. Nirwan, G. Roux, W. Hofstetter, and K. Le Hur, Phys. Rev. Lett. **120**, 157201 (2018).

[79] Y. Huang, X.-yu Dong, D. N. Sheng, and C. S. Ting, Phys. Rev. B **103**, L041108 (2021).

[80] C. N. Varney, K. Sun, V. Galitski, and M. Rigol, Phys. Rev. Lett. **107**, 077201 (2011).

[81] J. Carrasquilla, A. Di Ciolo, F. Becca, V. Galitski, and M. Rigol, Phys. Rev. B **88**, 241109(R) (2013).

[82] F. Verstraete and J. I. Cirac, arXiv:cond-mat/0407066.

[83] For a review on conformal field theories, see, e.g., P. Ginspary, Applied conformal field theory, arXiv:hep-th/9108028.

[84] R. Wang, Y. Wang, Y. X. Zhao, and B. Wang, Phys. Rev. Lett. **127**, 237202 (2021).

[85] Z. Nussinov and G. Ortiz, Proc. Natl. Acad. Sci. USA **106**, 16944 (2009).

[86] Z. Nussinov and G. Ortiz, Ann. Phys. **324**, 977 (2009).

[87] D. Gaiotto, A. Kapustin, N. Seiberg, and B. Willett, J. High Energy Phys. 02 (2015) 172.

[88] S. Bieri, C. Lhuillier, and L. Messio, Phys. Rev. B **93**, 094437 (2016).